Obstacle avoidance control design : an experimental evaluation in vehicle platooning

Document status and date:
Published: 01/09/2016

Document Version:
Accepted manuscript including changes made at the peer-review stage

Please check the document version of this publication:

• A submitted manuscript is the version of the article upon submission and before peer-review. There can be important differences between the submitted version and the official published version of record. People interested in the research are advised to contact the author for the final version of the publication, or visit the DOI to the publisher's website.
• The final author version and the galley proof are versions of the publication after peer review.
• The final published version features the final layout of the paper including the volume, issue and page numbers.

Link to publication

Download date: 17. Nov. 2023

Obstacle Avoidance Control Design: An Experimental Evaluation in Vehicle Platooning

M. Alirezaei, E. Semsar-Kazerooni & J. Ploeg
TNO, Department of Integrated Vehicle Safety, Automotive Campus 30, 5708 JZ Helmond, The Netherlands
E-mail: mohsen.alirezaei@tno.nl, elham.semsarkazerooni@tno.nl, jeroen.ploeg@tno.nl

ABSTRACT: In this paper, an obstacle avoidance controller (OA) based on the impedance control method is developed. The main goal of the OA controller is to guarantee robust gap making for a merging vehicle within a platoon of vehicles which are longitudinally automated. The proposed OA controller is developed in a simulation environment and later implemented and evaluated on test vehicles. Experimental results show the effectiveness of the proposed method for robust gap making and collision avoidance scenarios.

1 INTRODUCTION

Cooperative driving of highway vehicles has been identified as a promising strategy for autonomous or semi-autonomous vehicle control to enhance safety, improve traffic efficiency and increased fuel economy toward intelligent transportation systems(Semsar-Kazerooni 2015, Shladover 2013). Cooperative Adaptive Cruise Control (CACC) (Ploeg 2014, Milans 2014, Semsar-Kazerooni 2016) is an example of an automatic vehicle-following control system. CACC, using wireless communications for data exchange, allows a smaller inter-vehicle distance compared to adaptive cruise control (ACC). However, CACC in (Ploeg 2014) merely deals with safe inter-vehicle distance among the platoon member, in one lane. Extending cooperative driving to include maneuvering vehicles between the lanes is the next step towards automated driving (Alirezaei 2015). Therefore, an obstacle avoiding (OA) controller is necessary to see any object on the adjacent lanes as an obstacle and then to keep a safe distance to this obstacle. Different obstacle avoidance strategies are proposed in the literature. Many of these strategies are based on defining a potential function which becomes infinitely large, when the distance is too small. Therefore, the corresponding control action, i.e. the gradient of the potential function, would be infinitely large as the distance to obstacle decreases (Wolf 2008, Volpe 1990). This type of control action does not suit specific applications i.e. gap making for a merging vehicle. In this paper, an obstacle avoidance controller based on the impedance control strategy is proposed that aims at integrating existing CACC functionality with obstacle avoidance and gap making functionalities. The impedance control strategy, first proposed for robotic manipulator control, can be explained (Hogan 1985) by using a spring analogy to define virtual bumpers in 2D collision avoidance strategies. Using numerical simulations and experimental evaluation, we provide an assessment for the proposed OA controller. The paper is organized as follows: In Section 2 the platoon dynamics are presented. In Section 3 the OA controller design and proof of stability are shown. In Section 4 the simulation results are explained. In Section 5 and 6 the experimental results and conclusions are drawn.

2 PLATOON DYNAMICS

To investigate the behavior of the CACC and OA controllers on a platoon of vehicles, an appropriate model of a platoon is necessary. Consider the following dynamical model for vehicle i, $i = 1, ..., m$ in a platoon of m vehicles.

$$\begin{pmatrix} \dot{d}_{i-1|i} \\ \dot{v}_i \\ \dot{a}_i \end{pmatrix} = \begin{pmatrix} v_{i-1} - v_i \\ a_i \\ \frac{-1}{\tau} a_i + \frac{1}{\tau} u_i \end{pmatrix} \tag{1}$$

where $d_{i-1|i}$ is the distance between vehicle i and its preceding vehicle $i - 1$, v_i the longitudinal velocity of vehicle i, a_i the longitudinal acceleration of vehicle i, u_i is the external input (desired acceleration), and τ is a time constant representing drive-line dynamics. Here a homogeneous string of vehicles is assumed which means τ is vehicle independent. The objective of each vehicle in a platoon is to follow the preceding vehicle at a desired distance $d_{r,i-1|i}$ according to

$$d_{r,i-1|i}(t) = r_{i-1|i} + hv_i(t) \tag{2}$$

where h is the so called time gap and $r_{i-1|i}$ is the standstill distance between vehicle i and $i-1$. To regulate the inter-vehicle spaces to $d_{r,i-1|i}$, the spacing error e_i is then defined as

$$e_i(t) = d_{i-1|i}(t) - d_{r,i-1|i}(t) \tag{3}$$

The employed vehicle model in the control of the platoon is based on the vehicle model (1) and the spacing error e_i defined in (3). This model is represented as:

$$\begin{pmatrix} \dot{e}_i \\ \dot{v}_i \\ \dot{a}_i \end{pmatrix} = \begin{pmatrix} 0 & -1 & -h \\ 0 & 0 & 1 \\ 0 & 0 & \frac{-1}{\tau} \end{pmatrix} \begin{pmatrix} e_i \\ v_i \\ a_i \end{pmatrix} + \begin{pmatrix} 0 \\ 0 \\ \frac{1}{\tau} \end{pmatrix} u_i +$$

$$+ \begin{pmatrix} 0 & 1 & 0 \\ 0 & 0 & 0 \\ 0 & 0 & 0 \end{pmatrix} \begin{pmatrix} e_{i-1} \\ v_{i-1} \\ a_{i-1} \end{pmatrix} \tag{4}$$

3 PLATOON CONTROL

In this section, design of a CACC controller which deals with safe inter-vehicle distance in one lane and an OA controller which includes maneuvering vehicles between the lanes are discussed.

3.1 *CACC*

The main objectives for the platoon control problem are zero steady state for the spacing error, i.e. $\lim_{t\to\infty} e_i(t) = 0$, and string stability. These objectives are achieved with the help of a cooperative adaptive cruise controller (CACC) designed in (Ploeg 2011). Considering a one-vehicle look-ahead CACC, the input ξ_{ic} is defined such that

$$h\dot{u}_i = -u_i + \xi_{ic} \tag{5}$$

where the control law for ξ_{ic} is chosen as

$$\xi_{ic} = u_{i-1} + k_{pi}e_i + k_{di}\dot{e}_i \tag{6}$$

where k_{pi} and k_{di} are the proportional and derivative action gains of vehicle i for CACC controller, respectively, and the feedforward term u_{i-1} is obtained through wireless communication. Using (4) - (6), the following closed-loop system is thus obtained:

$$\begin{pmatrix} \dot{e}_i \\ \dot{v}_i \\ \dot{a}_i \\ \dot{u}_i \end{pmatrix} = \begin{pmatrix} 0 & -1 & -h & 0 \\ 0 & 0 & 1 & 0 \\ 0 & 0 & \frac{-1}{\tau} & \frac{1}{\tau} \\ \frac{k_{pi}}{h} & \frac{-k_{di}}{h} & -k_{di} & \frac{-1}{h} \end{pmatrix} \begin{pmatrix} e_i \\ v_i \\ a_i \\ u_i \end{pmatrix}$$

$$+ \begin{pmatrix} 0 & 1 & 0 & 0 \\ 0 & 0 & 0 & 0 \\ 0 & 0 & 0 & 0 \\ 0 & \frac{k_{di}}{h} & 0 & \frac{1}{h} \end{pmatrix} \begin{pmatrix} e_{i-1} \\ v_{i-1} \\ a_{i-1} \\ u_{i-1} \end{pmatrix}$$

or

$$\dot{z}_i = C_0 z_i + C_1 z_{i-1} \tag{7}$$

where $z_i = (e_i \ v_i \ a_i \ u_i)^T$ and the matrices C_0 and C_1 are defined, correspondingly. Ploeg (2011) has shown that for a bounded external input applied to the first vehicle and subject to some constraints on the controller gains, the above closed loop system will be exponentially stable. Figure 1 shows the block diagram of the CACC controller. where $G(s) = \frac{q_i(s)}{u_i(s)} = \frac{1}{s^2(\tau s+1)}$, $K(s) = k_{pi} + k_{di}s$, $D(s) = e^{-\theta s}$, θ is the communication delay and $q_i(s)$ is the Laplace transform of the vehicle i's position, $q_i(t)$. Here, u_i represents the entire external input implemented to vehicle i based on only the CACC control effort. In the next Section, the effect of the obstacle avoidance controller is explained.
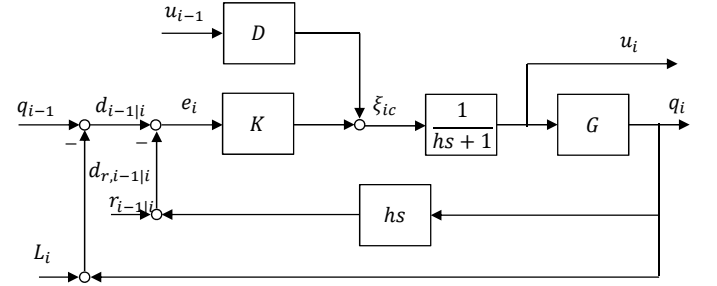

Figure 1: Block diagram of the controlled vehicles 2 and 4 of a platoon with CACC

3.2 *Obstacle Avoidance controller*

The Obstacle Avoidance (OA) controller is based on the impedance control approach. In this controller, virtual springs and dampers are connected to the merging car, which apply desired acceleration to the forward and backward platoon vehicles to realize the safe gap. Figure 2 shows the schematic of the OA controller in the gap making and merging maneuver. In this maneuver, vehicle 2 makes a gap for vehicle 4 who wants to merge into the platoon in front of vehicle 2. In this case, car 4 is responsible for making the gap between 4 and 1 (car 1 is driving in cruise control), whereas both car 2 and 4 are responsible for making the gap dis2MIOD. The control block diagram for vehicles 2 and 4 can be expressed as in Figure 3. Then, the controller u_i can be defined such that

$$h\dot{u}_i = -u_i + \xi_{ic} + \xi_{ioa} \tag{8}$$

where the control effort correspond to CACC, ξ_{ic}, is already defined in (6) and the control laws for the obstacle avoidance controller ξ_{ioa} for vehicles 2 and 4 are chosen as

$$\xi_{2oa} = k_{poar}(d_{24} - d_{r,24}) + k_{doar}(\dot{d}_{24} - \dot{d}_{r,24}) \tag{9}$$

$$\xi_{4oa} = k_{poaf}(d_{14} - d_{r,14}) + k_{doaf}(\dot{d}_{14} - \dot{d}_{r,14}) - \xi_{2oa} \tag{10}$$

where k_{poaf}, k_{doaf}, k_{poar} and k_{doar} are the proportional and derivative actions of the impedance controller which are regulating obstacle avoidance in vehicles 4 and 2, respectively. d_{ij} and $d_{r,ij}$ are the real
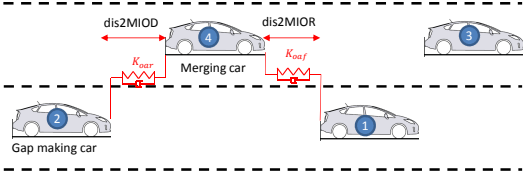
Figure 2: Vehicle topology in nominal merging scenario.

and desired projected distances between vehicle i and vehicle j, respectively.
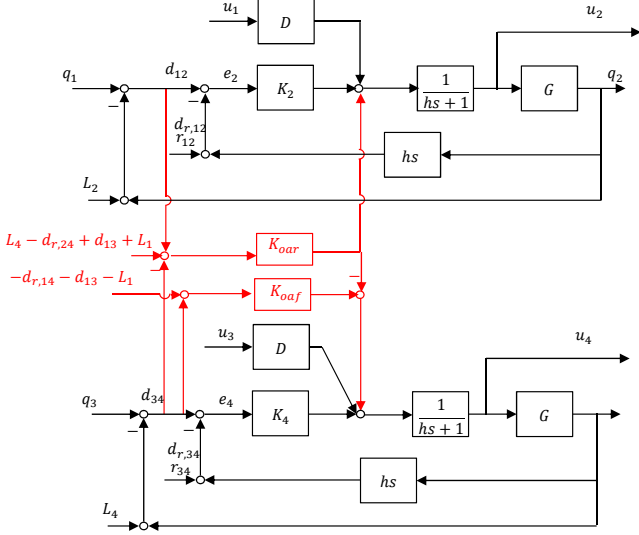

Figure 3: Block diagram of a controlled vehicle of a platoon with obstacle avoidance controller.

The distances d_{14} and d_{24} can be expressed by the following equations:

$$d_{14} = d_{34} - d_{13} - L_1 \tag{11}$$

$$d_{24} = d_{12} + d_{13} - d_{34} - L_4 + L_1 \tag{12}$$

where L_1 and L_4 are the length of the vehicle 1 and 4 respectively. By substituting (6) and (9) - (12) into (8) the following inputs thus obtained:

$$h\dot{u}_2 = -u_2 + u_1 + k_{p2}e_2 + k_{d2}\dot{e}_2 + k_{poar}(d_{12} + d_{13} - d_{34} - L_4 + L_1 - d_{r,24}) + k_{doar}(\dot{d}_{12} + \dot{d}_{13} - \dot{d}_{34}$$

$$-\dot{d}_{r,24}) \tag{13}$$

$$h\dot{u}_4 = -u_4 + u_3 + k_{p4}e_4 + k_{d4}\dot{e}_4 + k_{poaf}(d_{34} - d_{13} - L_1 - d_{r,14}) + k_{doaf}(\dot{d}_{34} - \dot{d}_{13} - \dot{d}_{r,14}) - k_{poar}(d_{12} + d_{13} - d_{34} - L_4 + L_1 - d_{r,24}) - k_{doar}(\dot{d}_{12}$$

$$+\dot{d}_{13} - \dot{d}_{34} - \dot{d}_{r,24}) \tag{14}$$

In order to generate the state space equations for the system of CACC and OA, it is necessary to add and subtract extra terms to (13) and (14)

$$h\dot{u}_2 = -u_2 + u_1 + k_{p2}e_2 + k_{d2}\dot{e}_2 + k_{poar}(d_{12} + d_{13} - d_{34} - L_4 + L_1 - d_{r,24}) + k_{doar}(\dot{d}_{12} + \dot{d}_{13} - \dot{d}_{34} - \dot{d}_{r,24})$$

$$-k_{poar}(d_{r,34} - d_{r,12}) + k_{poar}(d_{r,34} - d_{r,12}) \tag{15}$$

$$h\dot{u}_4 = -u_4 + u_3 + k_{p4}e_4 + k_{d4}\dot{e}_4 + k_{poaf}(d_{34} - d_{13} - L_1 - d_{r,14}) + k_{doaf}(\dot{d}_{34} - \dot{d}_{13} - \dot{d}_{r,14}) - k_{poar}(d_{12} + d_{13} - d_{34} - L_4 + L_1 - d_{r,24}) - k_{doar}(\dot{d}_{12} + \dot{d}_{13} - \dot{d}_{34} - \dot{d}_{r,24}) - k_{poaf}d_{r,34} + k_{poaf}d_{r,34} - k_{poar}(d_{r,34} - d_{r,12})$$

$$+k_{poar}(d_{r,34} - d_{r,12}) \tag{16}$$

Using (15) and (16) and the model of platoon dynamics (7) the state space equation for the closed loop system in the presence of both CACC and OA controllers, is obtained as

$$\dot{x}_i = A_0 x_i + A_1 x_{i-1} + B \tag{17}$$

where $x = [e_2 \ v_2 \ a_2 \ u_2 \ e_4 \ v_4 \ a_4 \ u_4]^T$ (see Appendix).

3.3 *Stability Analysis*

In this section, the stability of the proposed closed loop system is investigated. In equation 17 the B matrix only affects the steady state behavior and equilibrium point. Let's assume that vehicles 1 and 3 (the preceding vehicles) are in CACC mode and following a virtual reference vehicle. Returning to the platoon closed loop model eq. 17, the stability of the system of 4 vehicle only depends on the eigenvalue of the A_0 matrix. Considering the system with OA, assuming that CACC parameters are fixed, the eigenvalues are affected by four parameters, being k_{poaf}, k_{poar}, k_{doaf}, k_{doar}. Figure 4 shows the gain space (k_{poaf}, k_{poar}) versus the closed loop largest eigenvalue of the system where $k_{doaf} = k_{doar} = 0$. The red line shows the stability border where the $max(real(eig(A_0))) = 0$. Figure 5 shows the stability region for different damping ratios. The area below the lines shows the stable region. As it can be seen, increasing the damping of the OA controller yields a larger stability region.
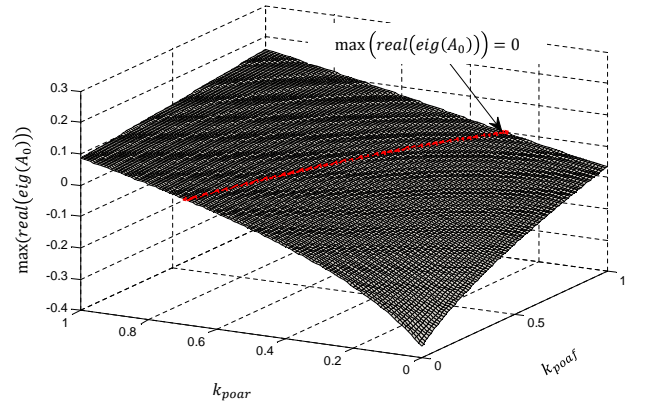

Figure 4: Eigen value of the system in the gain space(k_{poaf}, k_{poar})
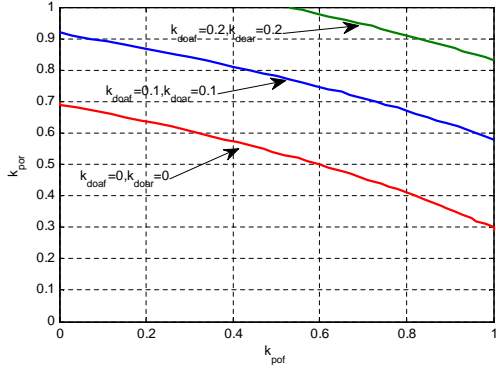
Figure 5: Stability region for different damping ratios, $k_{doaf} = k_{doar} = 0$ red line, $k_{doaf} = k_{doar} = 0.1$ green line, $k_{doaf} = k_{doar} = 0.2$ green line.

4   SIMULATION RESULTS

Several tests have been performed with the simulation environment to investigate the OA controller. However, here only the effect of initial conditions on the steady state behavior will be discussed. Figure 2 shows vehicle topology in the simulation where vehicles are driving with a speed of 80 km/h. We denote the distance from car 4 to the Most Important Object on the Right side and to the Most Important Object behind the host vehicle by $dis2MIOR$ and $dis2MIOD$, respectively (see Figure 2). The desired value of 10 m is considered for $dis2MIOR$ and $dis2MIOD$. Figure 6 shows the results for the first simulation where the initial distance of the car 4 with respect to car 1 is 5.5 m. As it can be seen, OA controller in car 4 applies smooth acceleration (lower subplot) and increases distance to car 1 (upper subplot). The controller on car 2 generates desired gap (middle subplot) for car 4 at the same time.
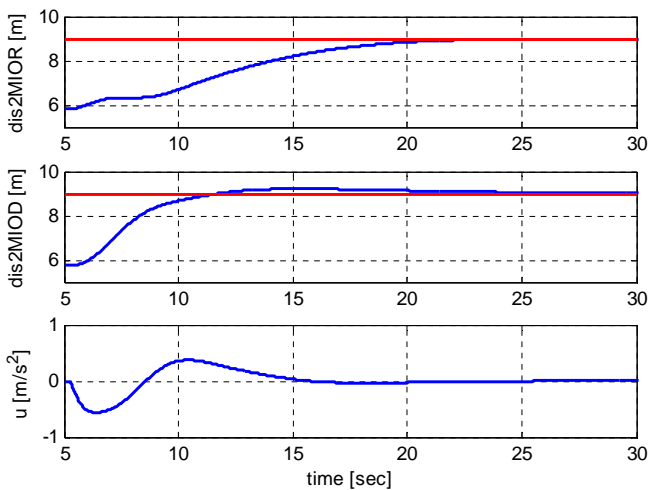

Figure 6: Simulation results for the merging car 4 with $d_{13} = 5.5m$, distance to the Most Important Object on the Right side (dis2MIOR) (upper subplot), distance to the Most Important Object behind the host vehicle(dis2MIOD) (middle subplot) and the control input (lower subplot) and red lines shows desired distance

Figure 7 shows the result for the second simulation where the initial distance of car 4 with respect to car 1 is 11m. As can be seen, the controller generates acceleration input (lower subplot) to adjust the distance between car 4 and car 1 (upper subplot).
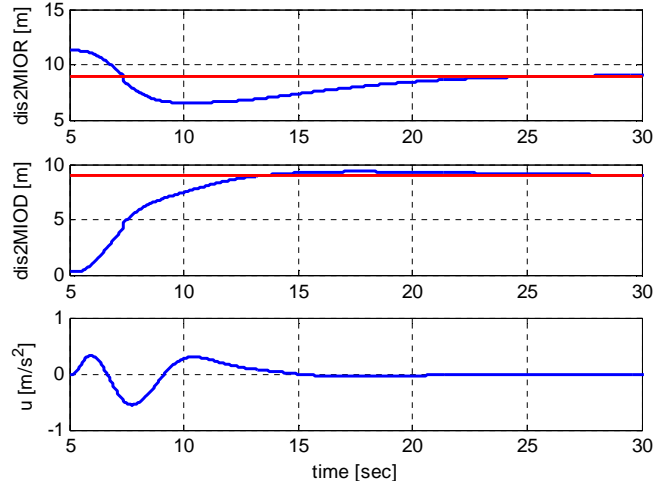

Figure 7: Simulation results for the merging car 4, distance to the Most Important Object on the Right side (dis2MIOR) (upper subplot), distance to the Most Important Object behind the host vehicle(dis2MIOD) (middle subplot) and the control input (lower subplot) and red lines shows desired distance

5   EXPERIMENTAL RESULTS

The proposed control strategy is experimentally evaluated by implementing it on a real time computer, in driving car laboratories (CarLabs). The CarLabs are TOYOTA Prius (Fig 8) which are equipped with a throttle and brake control system. Also the CarLabs are equipped with IEEE 802.11p-based wireless communication, allowing for communication of the desired vehicle acceleration at an update rate of 10 Hz. Furthermore, the CarLabs are equipped with environmental perception sensors like radar, camera and GPS. Using these sensors all CarLabs are able to measure dis2MIOR and dis2MIOD and their time derivatives. Several tests have been performed on a test track but for the sake of brevity only two sets of experiments will be shown. In both experiments all cars are driving at 45 km/h and the desired gap between cars is 10m. Figure 9 shows the vehicle configuration in the first experiment. In this experiment, car 4 is going to merge between car 1 and car 2. So car 2 should make a safe gap for the merging car. Simultaneously, car 4 should make a safe distance to car 1.
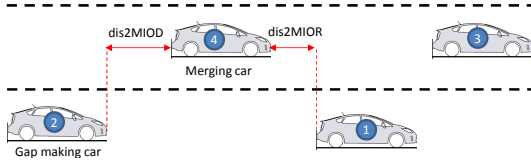

Figure 8: Carlab

Figure 9: Vehicle topology in the first experiment

Figure 10 shows that the OA controller provides smooth input (lower subplot) to the system and the dis2MIOR and dis2MIOD go to the desired value of 10m. The discontinuity in dis2MIOR around 32 sec is due to the environmental perception sensors which also has influence on the controller input.
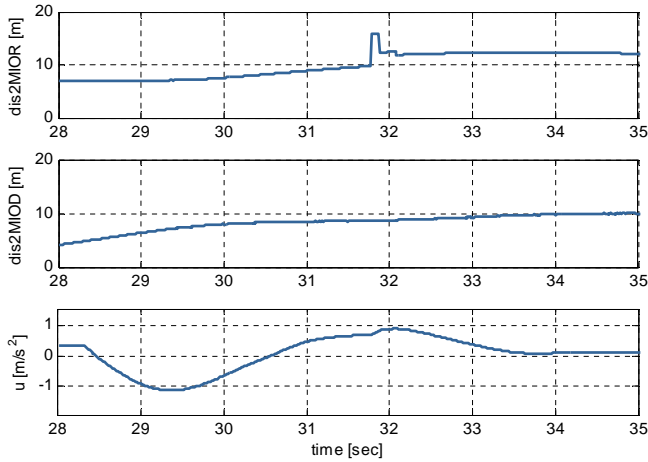

Figure 10: Experimental results for the merging car 4, distance to the Most Important Object on the Right side (dis2MIOR) (upper subplot), distance to the Most Important Object behind the host vehicle(dis2MIOD) (middle subplot) and the control input (lower subplot)

Figure 11 shows the vehicle configuration in the second experiment. The goal of this experiment is to investigate some special conditions on the controller performance. In this experiment, car 3 is going to merge between car 1 and car 2. In this case there is no car in front of car 3. Furthermore, car 4 is going to merge behind car 2 so there is no car behind the merging car. So car 2 on one hand should make a safe gap for car 3 and at the same time, car 4 should make a safe distance to the gap making car.

Figure 12 shows the $dis2MIOR$ and $dis2MIOD$ and control input for car 3. As it can be seen, the controller applies smooth input to the system and realizes 10m gap in front and behind the host vehicle. Figure 13 shows the $dis2MIOR$ and $dis2MIOD$ and control input for car 4. As it can be seen first the distance between car4 and car2 ($dis2MIOR$) due to the gap making for the car 3 decreases and as soon as the controller in car4 is activated, the controller realizes the safe distance to car2.

6 CONCLUSION

The problem of designing an obstacle avoidance controller based on the impedance control method for co-
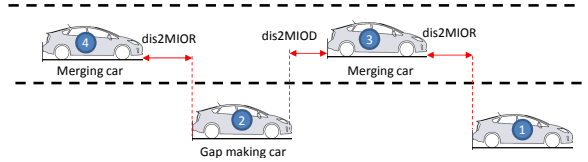

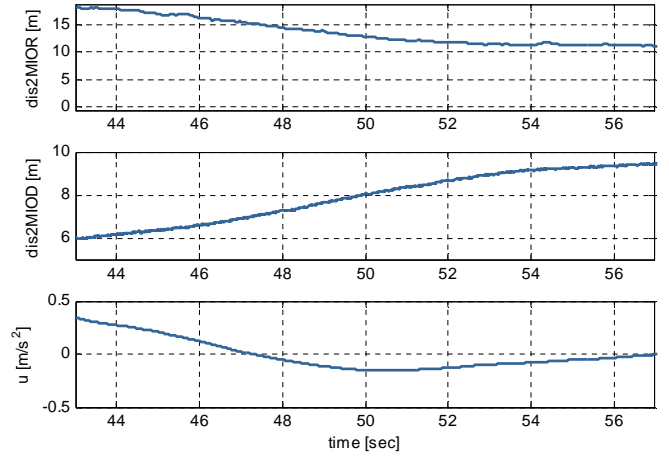Figure 11: Vehicle topology in the second experiment

Figure 12: Experimental results for the merging car 3, distance to the Most Important Object on the Right side (dis2MIOR) (upper subplot), distance to the Most Important Object behind the host vehicle(dis2MIOD) (middle subplot) and the control input (lower subplot)
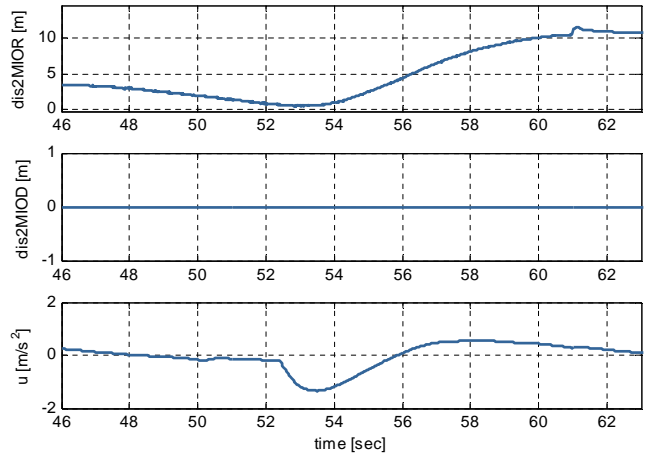

Figure 13: Experimental results for the merging car 4, distance to the Most Important Object on the Right side (dis2MIOR) (upper subplot), distance to the Most Important Object behind the host vehicle(dis2MIOD) (middle subplot) and the control input (lower subplot)

operative driving has been presented. The proposed system has been evaluated in simulation and also tested in experiments under a variety of maneuvers. It has been proven that the proposed OA controller is capable of generating a predefined gap between vehicles for a merging vehicle.

REFERENCES

Alirezaei, M. Jansen, S.T.H., Janssen, J.M., Experimental evaluation of collision avoidance system using state dependent Riccati equation technique. *24th International Sympo-*

sium on Dynamics of Vehicles on Roads and Tracks, Graz, Austria, 2015.

Hogan, N., Impedance control: an approach to manipulation. *ASME J. Dynamic Syst. Meas. Control*, 107:124, 1985.

Lidstrom, K., Sjoberg, K., Holmberg, U., Anderson J. and Bergh, F., A modular CACC system integration and design, *IEEE Trans. Intell. Transp. Syst.*, vol. 13, no. 3, pp. 1050-1061, Sep. 2012.

Milans, V., Shladover, S.E., Spring, J., Nowakowski, C., Kawazoe, H. and Nakamura, M., Cooperative adaptive cruise control in real traffic situations, *IEEE Trans. Intell. Transp. Syst.*, vol. 15, no. 1, pp. 296-305, Feb. 2014.

Ploeg, J., Scheepers, B.T.M., van Nunen, E., van de Wouw, N., and Nijmeijer, H., Design and Experimental Evaluation of Cooperative Adaptive Cruise Control, *IEEE Conference on Intell. Transp. Syst.*, Washington, USA, October 5-7, 2011.

Ploeg, J., Shukla, D.P., van de Wouw, N. and Nijmeijer, H., Controller Synthesis for String Stability of Vehicle Platoons, *IEEE Transactions on Intelligent Transportation Systems*, vol. 15, no. 2, April 2014.

Ploeg, J., van der Wouw, N. and Nijmeijer, H., $\mathcal{L}_p$ String stability of Cascaded Systems: Application to Vehicle Platooning", *IEEE Transactions on Control Systems Technology*, vol. 22, no. 2 March 2014.

Semsar-Kazerooni, E., Ploeg, J., Interaction protocols for cooperative merging and lane reduction scenarios, *18th IEEE International Conference on Intell. Transp. Syst.*, Las Palmas, 2015.

Semsar-Kazerooni, E., Verhaegh, J., Ploeg, J., Alriezaei, M., Cooperative Adaptive Cruise Control: An Artificial Potential Field Approach, *IEEE Intelligent Vehicles Symposium*, Gothenburg, Sweden, 2016.

Shladover, S. E., Su, D. and Lu, X. Y., Impacts of cooperative adaptive cruise control on freeway traffic flow, *Transportation Research Record: Journal of the Transportation Research Board*, vol. 2324, 2013.

Volpe R. and Khosla, P., Manipulator control with superquadric artificial potential functions: Theory and experiments, *IEEE Trans. Syst., Man, Cybern.*, vol. 20, no. 6, 1990.

Wolf M. and Burdick, J., Artificial potential functions for highway driving with collision avoidance, *IEEE Int. conf. on robotics and automation (ICRA)*, May 2008.

$$B = \begin{pmatrix} 0 \\ 0 \\ 0 \\ -\frac{-k_{poar}\,(r_{12}-r_{34})+k_{poar}\,(L_4+d_{r,24}-d_{13}-L_1)}{h} \\ 0 \\ 0 \\ 0 \\ -\frac{k_{poaf}\,(d_{r,14}+d_{13}+L_1)-k_{poaf}\,r_{34}+k_{poar}\,(r_{12}-r_{34})-k_{poar}\,(L_4+d_{r,24}-d_{13}-L_1)}{h} \end{pmatrix}$$

APPENDIX

$$\mathbf{A}_0 = \begin{pmatrix} 0 & -1 & -h & 0 & 0 & 0 & 0 & 0 \\ 0 & 0 & 1 & 0 & 0 & 0 & 0 & 0 \\ 0 & 0 & -\frac{1}{\tau} & \frac{1}{\tau} & 0 & 0 & 0 & 0 \\ \frac{k_{p2}+k_{poar}}{h} & -\frac{k_{d2}+k_{doar}-h\,k_{poar}}{h} & -k_{d2} & -\frac{1}{h} & -\frac{k_{poar}}{h} & \frac{k_{doar}-h\,k_{poar}}{h} & 0 & 0 \\ 0 & 0 & 0 & 0 & 0 & -1 & -h & 0 \\ 0 & 0 & 0 & 0 & 0 & 0 & 1 & 0 \\ 0 & 0 & 0 & 0 & 0 & 0 & -\frac{1}{\tau} & \frac{1}{\tau} \\ -\frac{k_{poar}}{h} & \frac{k_{doar}-h\,k_{poar}}{h} & 0 & 0 & \frac{k_{p4}+k_{poaf}+k_{poar}}{h} & -\frac{k_{d4}+k_{doaf}+k_{doar}-h\,k_{poaf}-h\,k_{poar}}{h} & -k_{d4} & -\frac{1}{h} \end{pmatrix}$$

$$A_1 = \begin{pmatrix} 0 & 1 & 0 & 0 & 0 & 0 & 0 & 0 \\ 0 & 0 & 0 & 0 & 0 & 0 & 0 & 0 \\ 0 & 0 & 0 & 0 & 0 & 0 & 0 & 0 \\ 0 & \frac{k_{d2}+k_{doar}}{h} & 0 & \frac{1}{h} & 0 & -\frac{k_{doar}}{h} & 0 & 0 \\ 0 & 0 & 0 & 0 & 0 & 1 & 0 & 0 \\ 0 & 0 & 0 & 0 & 0 & 0 & 0 & 0 \\ 0 & 0 & 0 & 0 & 0 & 0 & 0 & 0 \\ 0 & -\frac{k_{doar}}{h} & 0 & 0 & 0 & \frac{k_{d4}+k_{doaf}+k_{doar}}{h} & 0 & \frac{1}{h} \end{pmatrix}$$